21

# Powerful terahertz radiation source for studying the effects on protein conformation

© V.V. Teplyakov<sup>1</sup>, O.P. Cherkasova<sup>1,2,3</sup>, M.M. Nazarov<sup>1</sup>, M.R. Konnikova<sup>1,4</sup>, V.A. Tverdislov<sup>4</sup>, P.M. Gotovtsev<sup>1</sup>

- <sup>1</sup> National Research Center "Kurchatov Institute", Moscow, Russia
- <sup>2</sup> Institute of Automation and Electrometry, Siberian BranchRussian Academy of Sciences, Novosibirsk, Russia
- <sup>3</sup> Institute of Laser Physics of the Siberian Branch of Russian Academy of Sciences, Novosibirsk, Russia

e-mail: tepliakov.vv17@physics.msu.ru

Received December 12, 2024 Revised December 17, 2024 Accepted April 07, 2025

The effect of terahertz pulses with an energy of  $10\,\mu\text{J}$ , a peak field of 1.3 MV/cm, and a spectrum from 1 to 6 THz on protein (bovine serum albumin) was investigated. The protein pre-pressed into a pellet was irradiated. The exposure time was 15 min. After irradiation, the protein was dissolved in water at a concentration of 1 mg/mL. UV spectroscopy in the range of 220–360 nm revealed a decrease in the molar extinction coefficient, which can be interpreted as a sign of structural changes in protein molecules under irradiation with terahertz radiation with the specified parameters.

Keywords: intensive terahertz radiation, effects, albumin, UV spectroscopy.

DOI: 10.61011/EOS.2025.05.61656.22-25

## Introduction

The frequency range from 0.1 to 10 THz, is commonly referred to terahertz (THz) radiation [1,2]. The study of the interaction of THz radiation with biological objects is interesting due to the non-ionizing nature of the effect, the coincidence of radiation frequencies with the characteristic frequencies of vibrational-rotational modes of organic molecules and the frequencies of intermolecular vibrations [3,4]. The development of applications of THz radiation in biology and medicine is associated with the emergence of affordable sources of this type of radiation [5-8]. An intensive increase in the number of publications related to use of THz radiation for the study of biological objects has been observed since the nineties of the last century, which is associated with the discovery of new methods for generating and detecting THz radiation [9,10]. Nowadays the effect of THz radiation has already been shown at all levels of the organization of biological matter [11]: molecular [12,13], cellular [14,15], tissue [16,17] and organismic [18,19].

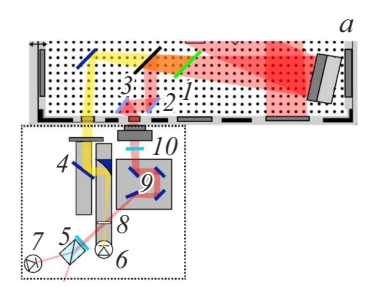
However, the variety of THz exposure conditions, model biological objects and methods of their analysis creates the problem of insufficient consistency and reproducibility of research results [9,20]. When studying the effects of THz radiation, it is necessary to pay attention to the following main categories of experimental conditions, which vary significantly in different studies and can have a critical impact on the result of each individual study, namely, exposure design, parameters of the irradiated biological object, its optical characteristics in the THz frequency range, as well as methods for analyzing the effect of exposure [3,9,14,21].

The design of the exposure is determined by the source of THz radiation and its characteristics, such as frequency spectrum of radiation, intensity, duration and frequency of pulses, spatial distribution, etc. Both monochromatic or narrowband and broadband radiation is used in terms of frequency. In the presence of modulation, the radiation is characterized by additional parameters such as pulse repetition rate, pulse duration, and peak intensity. The exposure mode refers to the presence of one or more cycles of THz exposure and their duration. The delivery of radiation to the sample is organized based on the optical characteristics of the media overcome by radiation and the need to comply with special conditions for biological samples [14,21].

The interaction of THz radiation with biological molecules, especially proteins, which perform important regulatory functions and are presented in significant quantities in cells and tissues of the body, can lead to a change in their activity and, as a result, to a change in the functions of cells and the body as a whole system [3,9,11]. Therefore, studying the effect of THz radiation on protein molecules is an urgent task.

A convenient model object of research is the globular protein albumin, which performs transport functions in human and animal blood. The single polypeptide chain of the serum albumin molecule, which has predominantly the  $\alpha$ -helix conformation, is folded into loops forming domains that are capable of reversibly binding various substances, including hormones, metal ions, fatty acids, etc. [22,23]. It has been shown that the albumin structure is labile, and conformational changes occur in it due to even relatively weak exposures [23], including THz radiation [12,24].

<sup>&</sup>lt;sup>4</sup> Moscow State University, Moscow, Russia



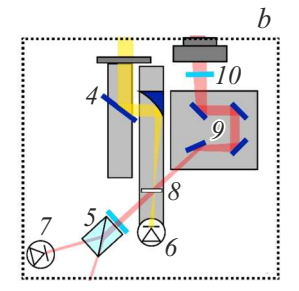


**Figure 1.** Installation diagram for generating THz radiation (yellow beam) from laser radiation (red beams) with detailed scheme of measurement of the duration of the THz pulse. (a) General view of the installation: I—LN crystal, 2—silicon mirrors, 3—optical beam divider. (b) Setup for measurement of the temporal shape of a THz pulse: 4—mirrors, 5—Wollaston prism, 6—Golay cell, 7—CCD camera, 8—an electro-optical detection crystal (when diagnosing radiation parameters) or a BSA sample (in an exposure experiment), 9—delay adjustment line, 10—polarizer.

Thus, the purpose of this paper was to study the interaction of intense, broadband pulsed THz radiation with bovine serum albumin (BSA) molecules.

The intense THz radiation was obtained by using the conversion of a femtosecond terawatt laser pulse in a thin plate of lithium niobate crystal (LiNbO<sub>3</sub>, LN) [25]. LN has high beam strength and non-linearity, and is also available as industrial plates of large area and small thickness [26]. High thresholds of optical breakdown and saturation in the LN crystal make it possible to use high laser pumping intensities, which quadratically increases the efficiency in the process of THz radiation generation. The large available area of the LN plates makes it possible to obtain a high total energy of a THz pulse from a multi-terawatt laser source [25].

## Materials and methods

#### Characteristics of the THz radiation source

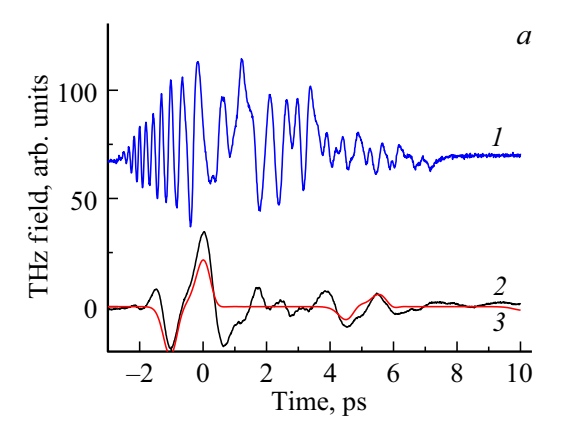
In this study we used a terawatt laser system installed at NRC "Kurchatov Institute" with the following parameters: energy on a LN crystal —  $250 \,\mathrm{mJ}$ , pulse repetition rate —  $10 \,\mathrm{Hz}$ , central wavelength —  $800 \,\mathrm{nm}$ , pulse duration —  $30 \,\mathrm{fs}$  (fig. 1, a).

THz radiation generation was optimised in the previous studies by choosing the optimal energy density (i.e., the beam size on the crystal) for the actual beam strength, which is  $60-120\,\mathrm{mJ/cm^2}$  (for 30 fs, 10 Hz and 800 nm), which corresponds to an intensity of  $2-4\,\mathrm{TW/cm^2}$  [25]. In addition, LN is one of the most widely used multifunctional crystals with many unique properties, including electrooptical, acoustico-optical, nonlinear optical, piezoelectric and ferroelectric properties. It is well suited for generating THz radiation due to the high value of the nonlinear optical coefficient [27], despite the strong absorption of

THz radiation in it. The non-synchronous generation of THz radiation in a thin backside layer of the crystal is an important difference between our THz source and traditional prisms with an tilted wavefront from LN. It allows, firstly, to obtain frequencies above 6 THz, and secondly, it is easy to adjust the duration and width of the THz radiation spectrum by stretching the optical pulse [25]. To ensure the optimal size of the laser beam on the LN, the radiation was "softly" pre-compressed by a spherical mirror with a focal length of 2.5 m and directed through a system of mirrors onto a crystal with a thickness of  $100 \,\mu\text{m}$ . The diameter of the converging beam was  $3 \,\text{cm}$ at the level of 1/e<sup>2</sup>. The generated, weakly converging THz radiation was delivered by mirrors to the sample and was further refocused by a short-focus parabolic mirror (f = 5 cm) either onto the sample (BSA pellet) or onto another nonlinear crystal (GaP) for detection of the duration (Fig. 1, b). The laser radiation passed through the LN crystal was removed from the THz beam by a special beam splitter on a thin substrate of crystalline quartz, transparent to THz radiation. The remnants of the unflected laser radiation (3%) were blocked with black polyethylene. The beam splitter reflected 97 % of the laser radiation energy, and after attenuation, this beam was used to measure the duration of the THz pulse. After the crystal detector (or after the BSA pellet), the transmitted THz radiation was measured by a Golay cell for energy control (Fig. 1, b).

Experimentally, it was found that when attempts were made to use a pulse with energies slightly lower than  $10\,\mu\rm J$ , there was no effect on the BSA, therefore pulses with such energy were used. It was technically possible to use higher THz energies, however, for better preservation of the LN crystal under prolonged irradiation (exposure time of 15 min), the above parameter was chosen.

A single-shot electro-optical detection (EOD) scheeme was created to measure the duration and spectrum of a THz pulse (Fig. 1, b) [28].  $100 \,\mu \text{m}$  thick GaP crystal was a detector (Fig. 1, designation 8) which for  $\lambda = 800 \, \text{nm}$ is capable of detecting THz radiation in the range from 0.05 to 7 THz without significant distortion. The oblique incidence of the probe beam relative to the THz beam on the EOD crystal turned the spatial scan (measured by the CCD camera) into a temporal scan, i.e. it showed the time profile of the THz pulse on the CCD camera in a single laser shot. The size of the THz beam aperture at the EOD crystall was 5 mm. This provided a measuring range of 5 ps with an angle of 20° between the beams. If necessary, the delay line 9 (Fig. 1) was used to move the measured time window (also to expand the measurement range by combining of several offset frames, as in Fig. 2, a for the interval 12 ps). Birefringence induced by THz pulses generated vertical polarization in the measured arm of the probe beam directed at the CCD camera. A fraction of vertical polarization (on the order of  $10^{-6}$ ) passed through the polarizer 10 for the optimal sensitivity. Negative values of the THz field looked like dark bands against this weak



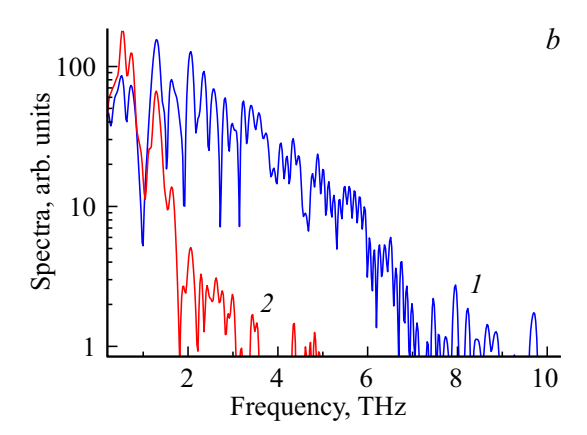


**Figure 2.** (a) Time profiles of THz pulses obtained for the case of laser radiation with a duration of 30 fs (1), 250 fs (2), modeling for the case of 250 fs (3); (b) respective spectra of THz pulses (1) and (2).

background (relative to the weak background), while the positive parts of the pulse field produced light bands.

The Fourier transform of the measured temporal form of a THz pulse was used to obtain a pulse spectrum (Fig. 2), an important feature of which is the presence of relatively high energies at high frequencies (after 3 THz), which was not achieved earlier in published papers studying powerful (>  $10 \mu J$ ) THz pulses. spectrum we measured continues up to 6 THz. The peak intensity of the THz field  $I_{\rm THz} \sim 0.6 \, {\rm W}/(w^2 \tau)$  [29] was 2.2 GW/cm<sup>2</sup>, where the half-height duration for the highfrequency case was  $\tau = 3$  ps (Fig. 2, a), energy  $W = 10 \,\mu\text{J}$ , focusing into a spot with an average (in frequency) radius  $w = 0.3 \,\mathrm{mm}$  at level  $1/\mathrm{e}^2$  (measured by the transmission of THz pulse energy through diafragm with diameters of  $0.5-1.5 \,\mathrm{mm}$ ). This corresponds to the magnitude of the THz field  $E_{\text{THz}}[\text{V/cm}] = 27.45(I_{\text{THz}}[\text{W/cm}^2])^{0.5}$  [29], in our case  $E_{\text{THz}} \approx 1.3 \, \text{MV/cm}$ .

The high value of the peak THz field was verified by THz pulse-induced transparency in semiconductors — a well-known method in the literature for z scanning [29,30]. In our case, p-doped silicon ( $n_e = 2.5 \cdot 10^{16} \, \mathrm{cm}^{-3}$ ) with the thickness of 270  $\mu$ m changed its transmittance in the position 8 (Fig. 1) from 10% in 1 cm from the THz beam waist to 16% in the THz radiation waist. Such induced transmission increase is possible only with a THz pulse with  $\mu$ J-energy, ps-duration, and submillimeter focusing, i.e. at fields greater than 1 MV/cm.

With the measured duration of the THz pulse, the expected single-period pulse was dispersed in both directions in time, and the total duration was about 5 ps. The blurring is related both to the dispersion of high THz frequencies in the LN crystal during generation, and to the dispersion in the detector crystal and in the divider. Blurring can be "turned off" by stretching the laser pulse to 250 fs, then all THz energy will be concentrated in the low frequency range of 0.2-1 THz, where the dispersion in all the materials we use is small. Thus, the peak THz field can be increased (for a low-frequency THz pulse in Fig. 2, a  $\tau \approx 1$  ps at

 $W=5\,\mu\mathrm{J},~E=1.6\,\mathrm{MV/cm})$ . But the maximum total THz energy is obtained with the shortest THz pulse. The model calculations (Fig. 2, red curve) took into account the dispersions and thicknesses of both crystals (generator and detector) [31,32]. The sensitivity spectrum of a GaP crystal with a thickness of  $100\,\mu\mathrm{m}$  is obviously wider than the range of 6 THz. By coincidence of the model and experiment, thicknesses, time profiles and spectra were refined, and the causes of THz pulse "blurring" over time were identified. The second pulse in the region of 5 ps is associated with generation on the incoming side of the LN.

### Sample preparation

BSA (Sigma-Aldrich, USA) was used in this research. The dry BSA sample was pressed using a hydraulic press at a pressure of 3t into pellets with a diameter of 13 mm and a thickness of  $290 \pm 27\,\mu m$ . The average pellet weight was  $5.7 \pm 0.5$  mg. The proportion of the irradiated substance was increased (an area of the order of  $2 \times 2$  mm was irradiated) by cutting out the middle of the pellet out  $(18-25\,\%$  of the initial mass, size  $4 \times 4$  mm) that was inserted into a special holder (Fig. 3), printed on a 3D printer, and placed in an experimental irradiation facility (Fig. 1). The center of the sample holder was aligned with the THz waist at the peak of the THz radiation passed through the empty arbor.

The irradiation time was 15 min. BSA samples prepared in the same way, but not exposed to radiation, were selected as control samples. Experimental and control samples were prepared on the day of irradiation. In total, three series of experiments were performed with three experimental and control samples in each series.

30 min after irradiation, the experimental and control samples were dissolved in bidistilled water with a concentration of 1 mg/mL. UV absorption spectra were recorded using ShimadzuUV-3600 spectrophotometer (Japan) in standard quartz cuvettes (optical path length 1 cm, volume 3 ml). Measuring range 200 – 350 nm. A cuvette with

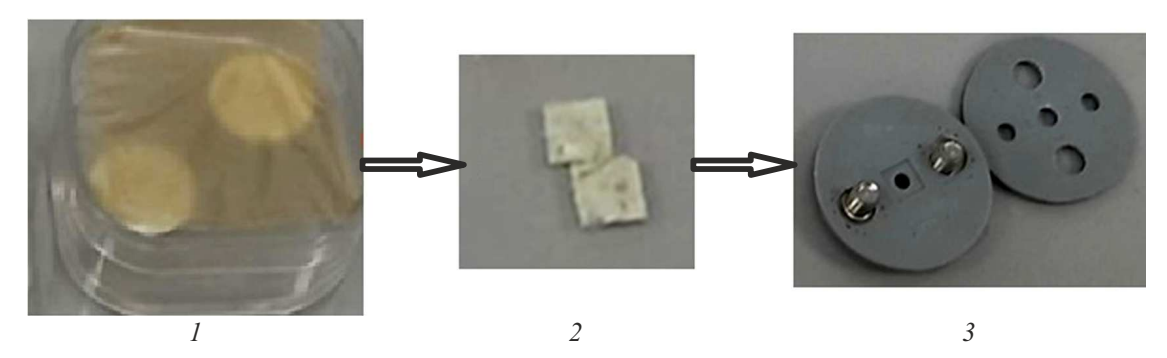


**Figure 3.** Sample preparation stages: (1) BSA pellets, (2) part of the pellet, (3) holder for irradiating part of the pellet.

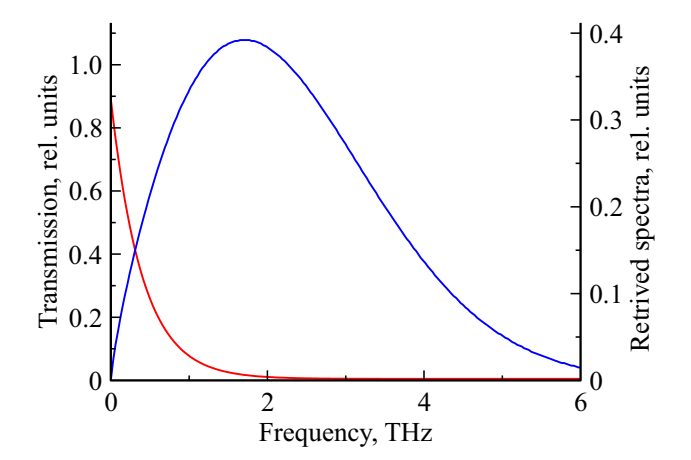


**Figure 4.** The calculated transmission spectrum of a  $300 \,\mu\text{m}$  thick BSA pellet (red curve) and the model spectrum of the THz source used (blue curve).

bidistilled water was placed in the reference channel. The results were presented as a dependence of the molar extinction coefficient on the wavelength.

## **Results and discussion**

A unique THz radiation source was used in this study to irradiate the protein, which has a wide spectrum (up to 6 THz at an energy of  $10 \mu J$ ) and an intensity of up to 3 GW/cm<sup>2</sup> [25]. The analysis of the dose received by the irradiated objects is of great importance when analyzing the effects of THz radiation [33,34]. It should be borne in mind that radiation can be reflected from an object, it can pass through an object and/or it can be absorbed by it. The thickness of the BSA pellet was selected in such a way that 90% of the incident radiation was absorbed. The data of the absorption of BSA pressed into pellets in the THz frequency range [35,36] were used for calculating the optimal pellet thickness which was  $300 \,\mu m$  (Fig. 4). The average pellet thickness was  $290 \pm 27 \,\mu \text{m}$  for the sample preparation. The total diameter of the THz beam was 2 mm, and a segment of a pellet of apropriate size was

placed in this area. Direct measurements of the transmitted THz radiation showed that about 10% of the THz pulse energy passes through the sample during irradiation, and this parameter does not change during irradiation within the measurement error, which is 3%. It follows from Fig. 4 that frequencies below 1 THz are not completely absorbed in the sample and can pass through it, frequencies of  $2-3\,\mathrm{THz}$  are completely absorbed throughout the depth, frequencies of  $4-6\,\mathrm{THz}$  can be absorbed only in the surface layer the sample.

It is possible to estimate the absorbed dose D taking into account the radiation absorbed by the BSA pellet, the size of the pellet, the irradiation time of  $t = 15 \,\text{min} \, (900 \,\text{s})$ , pulse repetition rate  $(10 \,\text{Hz})$ :

$$D = \frac{dE}{dm},$$

E is the absorbed energy, m is the body weight,

$$E=E_0-E',$$

 $E_0$  is the total incident energy on the sample, E' is the total energy elapsed,

$$\frac{E'}{E_0} = \frac{I'}{I_0}$$
 (from the Bouguer-Lambert-Baer law) = 0.1.

Then  $E = 0.9E_0$ ,  $E_0 = E_{01}N$ ,  $E_{01}$  is the energy of 1 pulse, N is their number,

$$N = ft = 10 \,\text{Hz} \cdot 900 \,\text{s} = 9000,$$

$$E = 0.9E_0 = 0.9E_{01}ft = 0.9 \cdot 10 \,\mu\text{J} \cdot 10 \,\text{Hz} \cdot 900 \,\text{s}$$

$$= 81 \,\text{mJ},$$

$$D = \frac{dE}{dm} = \frac{81 \,\text{mJ}}{1.25 \,\text{mg}} = 64.8 \,\frac{\text{mJ}}{\text{mg}}.$$

Based on the above calculations, the absorbed energy was 81 mJ, and the absorbed dose was 64.8 kJ/kg. When irradiating cells, tissues, and organisms in the THz frequency range, it is difficult to estimate the absorbed dose [33], especially since there are currently no generally accepted

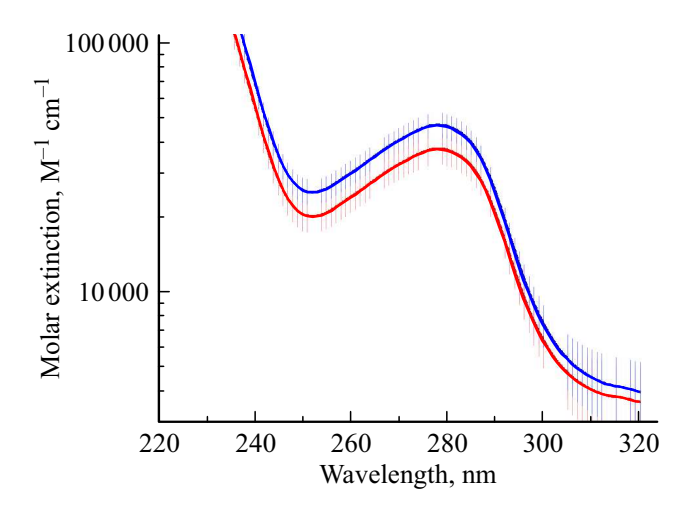


**Figure 5.** Molar extinction coefficients of BSA solutions before (blue line) and after irradiation (red line). The relative errors are calculated for three independent measurements.

safe radiation doses developed for the THz range [3,6,9]. This is attributable to the fact that the mechanisms of interaction of THz radiation with biological objects are not yet well understood. When evaluating the effects of THz radiation, the magnitude of the incident radiation intensity is usually used. In our case, this value is 70 mW/cm<sup>2</sup>. International standards developed by the International Commission for Protection against Non-Ionizing Radiation for electromagnetic radiation with a frequency not exceeding 300 GHz are based on an assessment of thermal effects and establish an intensity level of 1 mW/cm<sup>2</sup> as safe [37]. There are no established limits for irradiation of biological objects above 300 GHz. The developed restrictions apply only to laser radiation, where, depending on the type of laser radiation, the safety limits are in the range from 1 to 100 mW/cm<sup>2</sup> [3,33].

The UV absorption spectrum of BSA has two absorption bands of different intensity in the range of  $200 - 350 \,\mathrm{nm}$ . The first, most intense band in the region of 200-220 nm is attributable to the presence of a large number of amide groups in the composition of peptide bonds. The second, less intense absorption band of 278 nm is determined by the contribution of aromatic amino acids tryptophan and tyrosine to absorption [23]. A change in the conformation of albumin is reflected in a change in the absorption characteristics of this particular band. Fig. 5 shows the dependence of the molar extinction coefficient on the wavelength for irradiated and control samples. The shape of the spectrum coincides with the BSA spectrum reported earlier [12]. The greatest differences in the amplitude of the spectra are observed at wavelengths of 250 and 278 nm. In three independent series of measurements (3 irradiated samples in each series), the qualitative of increased tramsmission effect of the irradiated sample relative to the control sample was repeated by an amount of the order of  $3 \cdot 10^3 \,\mathrm{M}^{-1} \,\mathrm{cm}^{-1}$ .

The absorption of the irradiated protein decreases in this study relative to the absorption of non-irradiated BSA in the range of 220-320 nm. It was shown in Ref. [12,38,39] that when dry BSA preparations are irradiated with continuous radiation with a frequency of 3.67 THz and an intensity of 20 mW/cm<sup>2</sup> for 60 min, the absorption of BSA increases at a wavelength of 278 nm. The change in albumin absorption is associated with a change in its conformation after irradiation [12,24]. At the same time, there were no noticeable differences in the amplitudes of the spectra at a wavelength of 250 nm. At the same time, when irradiating the same BSA sample with broadband pulsed THz radiation in the range 0.05–1.3 THz, with an average power of 150 nW, a pulse repetition rate of 80 MHz and a pulse duration of 2.5 ps [40], there is a decrease in the absorption amplitude at a wavelength of 250 nm compared with non-irradiated drugs. At the same time, an increase in the absorption of the irradiated protein is observed at a wavelength of 278 nm, as in the case of continuous radiation with a frequency of 3.67 THz. It is believed that the wavelength of 250 nm is responsible for the absorption of 17 disulfide bonds in the BCA molecule [23], which determine the mobility of its globule. Quantum chemical modeling has shown that these structures in the BSA molecule can participate in conformational transitions under the action of THz radiation [24,41].

A decrease in the amplitude of UV absorption, as in the present work, was observed in the spectrum of irradiated BSA when irradiating dry BSA preparations in a special cell with a free electron laser with a frequency of 2.3 THz, a pulse repetition frequency of 5.6 MHz, a pulse duration of 50 ps, a power of 250 mW, and an irradiation time of 9 min [42]. After irradiation, the BSA preparation was dissolved in water at a concentration of 1 mg/mL. A comparison of our results with previously reported data on the irradiation of BSA molecules is shown in the table.

As can be seen from the table, a difference in the effects of continuous and pulsed THz radiation on BSA molecules is observed: the UV absorption increases at a wavelength of 278 nm in case of exposure to a continuous laser with a frequency of 3.67 THz, a decrease in protein absorption is observed at this wavelength in case of exposure to a powerful pulsed THz radiation source used in this study and in Ref. [42]. A decrease in the IR absorption of BSA samples after irradiation was shown in the same study. The samples were placed in special cuvettes with fluoroplastic windows transparent to THz and IR radiation. The experimental setup was constructed in such a way that the IR spectrum was first recorded, then the sample was irradiated and the IR spectrum was recorded again, i.e. each irradiated sample was for itself and the control. This approach minimizes errors when studying the effects of exposure. Examples of combining THz irradiation and registration of effects in one experimental scheme are described, for example, recording of fluorescence [43] or the use of highly sensitive X-ray crystallography to determine

№	Δν,THz	f, MHz	$\tau_p$ , pc	Iav, mW/cm <sup>2</sup>	t, min	Effect	Link
1	1 – 6	$10^{-5}$	3	70	15	Reduction of UV absorption at 250 and 278 nm	This study
2	2.3	5.6	50	35	9	Reduction of UV absorption at 278 nm	[42]
3	0.05 – 1.3	80	2.5	$2.1 \cdot 10^{-3}$	30	Reduction of UV absorption at 250 nm, increase by 278 nm	[40]
4	0.2 - 1.5	80	3	$50 \cdot 10^{-6}$	60	Increasing the number of binding centers according to EPR spectroscopy data	[24,41]
5	3.67	_	_	20	60	Increase of UV absorption at 278 nm, reduction of the binding constant of BSA	[38,39] [12]

Parameters of THz radiation and effects on BSA

Note:  $\Delta v$  is the spectral range, f is the pulse repetition rate,  $\tau_p$  is the pulse duration,  $I_{av}$  is the average radiation intensity, t is the exposure time.

changes in protein structure during irradiation [44]. This allows observing the effects of THz exposure in real time.

The changes we observed in the spectra of the irradiated BSA are not related to thermal effects, since the estimated temperature change of the sample during irradiation with these parameters does not exceed 0.4 °C. It was previously shown that heating of BSA samples to 50 °C did not cause similar changes in the UV absorption spectra [38.42].

It should be noted that different BSA irradiation protocols were used in the above studies. In a number of articles, dry BSA powder was placed in an open conical tube, and radiation was applied from the top [12,40]. Special cuvettes for dry powder were used in another experiment [42]. BSA films deposited from an aqueous solution on a quartz substrate were irradiated in a number of studies [24,38,39,41]. BSA irradiation in the form of a pressed pellet makes it possible to calculate the radiation dose more accurately.

In this study we used one of the simplest methods for detecting the effects of THz irradiation, namely the registration of UV absorption spectra. It was previously shown that an increase in UV absorption under the action of THz radiation was accompanied by a decrease in the fluorescence signal and the binding ability of BSA [12], as well as changes in the circular dichroism spectra [12,45], i.e., they were confirmed by methods more sensitive to conformational modifications. Thus, the changes we observed in the UV absorption spectra of BSA when irradiated with an intense THz radiation source confirm the presence of conformational changes.

## Conclusion

This paper presents the first results of using a unique source of high-power and broadband THz radiation to study the interaction of this type of radiation with biological objects. THz radiation was generated by choosing an original method for non-synchronous pumping of a thin lithium niobate crystal near the breakdown threshold. A study was conducted on the effect of pulses with an

energy of  $10\,\mu\text{J}$ , a peak field of 1.3 MV/cm and a wide spectrum from 1 to 6 THz on BSA pressed into pellets. The exposure time was 15 min. The impact is non-thermal, as the calculated temperature increase was  $0.4\,^{\circ}\text{C}$ . After irradiation, the protein was dissolved in water at a concentration of 1 mg/ml. UV spectroscopy showed a decrease in the molar extinction coefficient at wavelengths between 250 and 278 nm, which is associated with a change in protein conformation during irradiation. A comparison is made with the available literature data. Differences in the BSA response to continuous and pulsed THz radiation are revealed.

### **Funding**

The study was carried out partly as part of the state assignment of the National Research Center "Kurchatov Institute", topics 2P.1 and 2F.4.2 (generation of THz radiation, conducting experiments), partly as part of the state assignment of the Institute of Automation and Electrometry of SB RAS (FWNG-2024-0025) and the Institute of Laser Physics of SB RAS (FWGU-2026-0005) (analysis of experimental data).

#### Conflict of interest

The authors declare that they have no conflict of interest.

## References

- Y.-S. Lee. Principles of terahertz science and technology (Springer-Verlag, USA, 2009).
   DOI: 10.1007/978-0-387-09540-0
- [2] S.-C. Zhang, D. Shu. *Terahertz photonics* (Institute of Computer Research, Moscow-Izhevsk, 2016), pp. 334 (in Russian).
- [3] O.P. Cherkasova, D.S. Serdyukov, A.S. Ratushnyak, E.F. Nemova, E.N. Kozlov, Yu.V. Shidlovsky, K.I. Zaitsev, V.V. Tuchin. Opt. i spektr., 128 (6), 852 (2020) (in Russian). DOI: 10.21883/OS.2020.06.49420.51-20

- [4] O.A. Smolyanskaya, N.V. Chernomyrdin, A.A. Konovko, K.I. Zaytsev, I.A. Ozheredov, O.P. Cherkasova, M.M. Nazarov, J. P. Guillet, S.A. Kozlov, Yu.V. Kistenev, J.L. Coutaz, P. Mounaix, V.L. Vaks, J.H. Son, H. Cheon, V.P. Wallace, Yu. Feldman, I. Popov, A.N. Yaroslavsky, A.P. Shkurinov, V.V. Tuchin. Prog. Quant. Electron., 62, 1 (2018). DOI: 10.1016/j.pquantelec.2018.10.001
- [5] V.L. Bratman, A.G. Litvak, E.V. Suvorov. UFN, 181 (8), 867 (2011) (in Russian). DOI: 10.3367/UFNr.0181.201108f.0867
- K.I. I.N. Dolganova, N.V. Zavtsev. Chernomyrdin. G.M. Katyba, A.A. Gavdush, O.P. Cherkasova, G.A. Komandin, M.A. Shchedrina, A.N. Khodan, D.S. Ponomarev, I.V. Reshetov, V.E. Karasik, M. Skorobogatiy, V.N. Kurlov, V.V. Tuchin. J. Opt., 22, 013001 (2020). DOI: 10.1088/2040-8986/ab4dc3
- [7] X. Chen, H. Lindley-Hatcher, R.I. Stantchev, J. Wang,
   K. Li, A.H. Serrano, Z.D. Taylor, E. Castro-Camus,
   E. Pickwell-MacPherson. Chem. Phys. Rev., 3, 011311 (2022). DOI: 10.1063/5.0068979
- [8] A.I. Nikitkina, P. Bikmulina, E.R. Gafarova, N.V. Kosheleva, Y.M. Efremov, E.A. Bezrukov, D.V. Butnaru, I.N. Dolganova, N.V. Chernomyrdin, O.P. Cherkasova, A.A. Gavdush, P.S. Timashev. J. Biomed. Opt., 26 (4), 043005 (2021). DOI: 10.1117/1.JBO.26.4.043005
- [9] O.P. Cherkasova, D.S. Serdyukov, E.F. Nemova, A.S. Ratushnyak, A.S. Kucheryavenko, I.N. Dolganova, G. Xu, M. Skorobogatiy, I.V. Reshetov, P.S. Timashev, I.E. Spektor, K.I. Zaytsev, V.V. Tuchin. J. Biomed. Opt., 26 (9), 090902 (2021). DOI: 10.1117/1.JBO.26.9.090902
- [10] V.L. Bratman, A.G. Litvak, E.V. Suvorov. TVT, 56 (5), 814 (2018) (in Russian). DOI: 10.31857/S004036440003379-0
- [11] V. Fedorov, S. Popova, A. Pisarchik. Int. J. Infrared Millim. Waves, 24 (8), 1235 (2003). DOI: 10.1023/A:1024801304083
- [12] O.P. Cherkasova, V.I. Fedorov, E.F. Nemova, A.S. Pogodin. Opt. i spektr., 107 (4), 565 (2009) (in Russian).
- [13] L. Wei, L. Yu, H. Jiaoqi, H. Guorong, Z. Yang, F. Weiling. Frontiers in Laboratory Medicine, 2 (4), 127 (2018). DOI: 10.1016/j.flm.2019.05.001
- V.I. Fëdorov, D.S. Serdyukov, O.P. Cherkasova, S.S. Popova,
   E.F. Nemova. J. Opt. Technol., 84 (8), 509 (2017).
   DOI: 10.1364/JOT.84.000509.
- [15] S. Romanenko, R. Begley, A.R. Harvey, L. Hool, V.P. Wallace.
   J. R. Soc. Interface, 14 (137), 20170585 (2017).
   DOI: 10.1098/rsif.2017.0585
- [16] I.V.A.K. Reddy, S. Elmaadawy, E.P. Furlani, J.M. Jornet. Sci. Rep., 13, 4643 (2023). DOI: 10.1038/s41598-023-41808-9
- [17] W. Liu, Y. Lu, R. She, G. Wei, G. Jiao, J. Lv, G. Li. Appl. Sci., 9 (5), 917 (2019). DOI: 10.3390/app9050917
- [18] V.I. Fedorov, N.Ya. Weisman, E.F. Nemova, A.A. Mamrashev, N.A. Nikolaev. Biophysics, **58** (6), 1043 (2013) (in Russian).
- [19] N.P. Bondar, I.L. Kovalenko, D.F. Augustinovich, A.G. Khamoyan, N.N. Kudryavtseva. Byul. eksp. biol. i med., 145 (4), 378 (2008) (in Russian).
- [20] H. Hintzsche, H. Stopper. Crit. Rev. Environ. Sci. Technol., 42, 2408 (2012). DOI: 10.1080/10643389.2011.574206
- [21] D.S. Serdyukov, T.N. Goryachkovskaya, I.A. Mescheryakova, S.V. Bannikova, S.A. Kuznetsov, O.P. Cherkasova, V.M. Popik, S.E. Peltek. Biomed. Opt. Express, 11 (9), 5258 (2020). DOI: 10.1364/BOE.400432
- [22] M.N. Komarova, YU.A. Gryzunov. *Al'bumin syvorotki krovi* v *klinicheskoj medicine* (Geotar, M., 1998), p. 28–51 (in Russian).

- [23] G.E. Dobrecov, YU.I. Miller. Al'bumin syvorotki krovi v klinicheskoj medicine (Irius, M., 1994), p. 11–28 (in Russian).
- [24] E.F. Nemova, O.P. Cherkasova, N.A. Nikolaev, G.G. Dultseva. Biofizika, 65 (3), 486 (2020) (in Russian). DOI: 10.31857/S0006302920030072
- [25] M.M. Nazarov, P.A. Shcheglov, V.V. Teplyakov, M.V. Chashchin, A.V. Mitrofanov, D.A. Sidorov-Biryukov, V.Y. Panchenko, A.M. Zheltikov. Opt Lett., 46 (23), 5866 (2021). DOI: 10.1364/OL.434759
- [26] M.V. Tsarev. Generaciya i registraciya teragercovogo izlucheniya ul'trakorotkimi lazernymi impul'sami. Uchebnoe posobie (Nizhegorodskij gosuniversitet, Nizhnij Novgorod, 2011), p. 75 (in Russian).
- [27] M.N. Palatnikov, A.V. Kadetova, M.V. Smirnov, O.V. Sidorova,
   D.A. Vorobev. Opt. Mater., 131, 112631 (2022).
   DOI: 10.1016/j.optmat.2022.112631
- [28] J. Shan, A.S. Weling, E. Knoesel, L. Bartels, M. Bonn, A. Nahata, G.A. Reider, T.F. Heinz. Opt. Lett., 25, 426-428 (2000). DOI: 10.1364/OL.25.000426
- [29] O.V. Chefonov, A.V. Ovchinnikov, S.A. Romashevskiy, X. Chai, T. Ozaki, A.B. Savel'ev, M.B. Agranat, V.E. Fortov. Opt. Lett., 42, 4889–4892 (2017). DOI: 10.1364/OL.42.004889
- [30] Y. Zhang, K. Li, H. Zhao. Front. Optoelectron., 14, 4–36 (2021). DOI: 10.1007/s12200-020-1052-9
- [31] M.M. Nazarov, A.P. Shkurinov, A.A. Angeluts, D.A. Sapozhnikov. Izvestiya vuzov. Radiofizika, 52 (8), 595 (2009) (in Russian).
- [32] A. Schneider, M. Neis, M. Stillhart, B. Ruiz, R.U.A. Khan, P. Günter. J. Opt. Soc. Am. B, 23 (9), 1822 (2006). DOI: 10.1364/JOSAB.23.001822
- [33] T. Kleine-Ostmann, C. Jastrow, K. Baaske, B. Heinen, M. Schwerdtfeger, U. Kärst, H. Hintzsche, H. Stopper, M. Koch, T. Schrader. IEEE Trans. Terahertz Sci. Technol., 4 (1), 12 (2014). DOI: 10.1109/TTHZ.2013.2293115
- [34] M.-O. Mattsson, O. Zeni, M. Simko. J. Infrared Millimeter Terahertz Waves, 39 (9), 863 (2018). DOI: 10.1007/s10762-018-0483-5
- [35] O.P. Cherkasova, M.M. Nazarov, A.P. Shkurinov, V.I. Fedorov. Radiophys. Quantum Electron., 52 (7), 518 (2009).
- [36] M. Nazarov, A. Shkurinov, V.V. Tuchin, X.-C. Zhang. In: Handbook of Photonics for Biomedical Science, ed. by V.V. Tuchin (CRC Press, Boca Raton, 2010), vol. 23, p. 519-617.
- [37] Guidelines for limiting exposure to electromagnetic fields (100 kHz to 300 GHz). International Commission on Non-Ionizing Radiation Protection (ICNIRP). Health Phys., 118 (5), 483-524 (2020). DOI: 10.1097/HP.0000000000001210
- [38] A.V. Kapralova, A.S. Pogodin. Vestnik NGU. Ser. Fizika, **5** (4), 182 (2010) (in Russian).
- [39] A.S. Pogodin, A.V. Kapralova. Millimetrovye volny v biologii i medicine, 3, 18 (2011) (in Russian).
- [40] V.I. Fedorov, A.S. Pogodin, V.G. Bespalov, S.E. Putilin, O.A. Smolyanskaya, Ya.V. Grachev, S.A. Kozlov. Millimetrovye volny v biologii i medicine, **3**, 50 (2009) (in Russian).
- [41] E.F. Nemova, T.V. Kobzeva, G.G. Dultseva, Russ. J. Phys. Chem. B, 18, 95 (2024). DOI: 10.1134/S1990793124010354
- [42] N.L. Lavrik, E.F. Nemova. Vestnik NGU. Ser. Fizika, 2 (4), 96 (2007) (in Russian).

- [43] G. Kaur, X.-C. Zhang. *Terahertz biomedical science and technology*, ed. by J.-H. Son (CRC Press, Boca Raton, 2014), p. 211–240.
- [44] I.V. Lundholm, H. Rodilla, W.Y. Wahlgren, A. Duelli, G. Bourenkov, J. Vukusic, R. Friedman, J. Stake, T. Schneider, G. Katona. Struct. Dyn., 2 (5), 054702 (2015). DOI: 10.1063/1.4931825
- [45] V.M. Govorun, V.E. Tretiakov, N.N. Tulyakov, V.B. Fleurov, A.I. Demin, A.Yu. Volkov, V. Batanov, A.B. Kapitanov. Int. J. Infrared and Millimeter Waves, 12, 1469 (1991).

Translated by A.Akhtyamov